# Real-time simulation and control systems design by the Response Surface Methodology and designed experiments

P. STEWART†*, P. J. FLEMING‡ and S. A. MACKENZIE§

*This paper examines two cases where the fitting of a model to experimental data makes possible the solution of extremely difficult design and simulation problems. In the first (aerospace) case, designed experiments were conducted on a permanent magnet AC motor which provided the motive power for a flight surface actuator in a more electric aircraft application. The Response Surface Methodology is applied to the measured data to achieve inclusion of the component in a real-time distributed aircraft simulation. In the second (automotive) case, oscillatory acceleration responses are controlled via an electronically actuated (drive by wire) throttle. Designed experiments were conducted on the test vehicle to achieve a systematic excitation of the vehicle driveline. An approximation to the measured data is achieved by the Response Surface Methodology allowing a controller to be designed extremely rapidly.*

## 1. Introduction

The applications of data-driven modelling described in this paper are associated with large amounts of data which are the products of designed experiments. The availability of increased computing power allows novel modelling of dynamic systems to be accomplished, often a necessity when other modelling and control methods have been tried and found to be unsuccessful. In both cases presented here, response surfaces associated with multivariable inputs are fitted to experimental data. The practical requirements that drive the development of this data modelling technique are in the one case the necessity to integrate a model of a permanent magnet AC (PMAC) motor powered actuator into a real-time distributed simulation environment, and in the other case, the development of a dynamic vehicle model in the context of rapid control system prototyping.

The versatility and tractability of the approach is confirmed by experiment, showing the wide range of application to both real-time control systems and real-time distributed simulation systems. The use of designed experiments to collect appropriate data across the operating envelopes of both systems provides the foundation of the response surface fitting approach.

## 2. Response Surface Methodology (RSM)

The Response Surface Methodology (RSM) (Myers and Montgomery 1995) is a technique designed to optimize process control by the application of designed experiments in order to characterize a system. The relationship between the response variable of interest ($y$) and the predictor variables ($\xi_1, \xi_2, \ldots, \xi_k$) may be known exactly allowing a description of the system of the form

$$y = g(\xi_1, \xi_2, \ldots, \xi_k) + \epsilon, \tag{1}$$

where $\epsilon$ is the model error and includes measurement error and other variability such as background noise. The error will be assumed to have a normal distribution with zero mean and variance $\sigma^2$. In general, the experimenter approximates the system function $g$ with an empirical model of the form

$$y = f(\xi_1, \xi_2, \ldots, \xi_k) + \epsilon, \tag{2}$$

† Electrical Machines Machines and Drives Group, Department of Electrical Engineering, University of Sheffield, Mappin Street, Sheffield S1 3JD, UK.

‡ Department of Automatic Control and System Engineering, University of Sheffield, Sheffield, UK.

§ QinetiQ Ltd, UK.

* To whom correspondence should be addressed.
e-mail: p.stewart@sheffield.ac.uk

where $f$ is a generally a polynomial of order three or less. This is the empirical or response surface model. The variables are known as natural variables since they are expressed in physical units of measurement. In the applications under consideration here, the natural variables are gearbox transfer ratio and road speed in the automotive case, and instantaneous torque and rotor velocity in the aerospace case. In the RSM, the natural variables are transformed into coded variables $x_1, x_2, \ldots, x_k$, which are dimensionless, zero mean and the same standard deviation. The response function now becomes

$$\eta = f(x_1, x_2, \ldots, x_k). \tag{3}$$

The successful application of RSM relies on the identification of a suitable approximation for $f$. It can for example be a first-order model of the form

$$\eta = \beta_0 + \beta_1 x_1 + \beta_2 x_2 + \cdots + \beta_k x_k. \tag{4}$$

This is often termed the main effects model since it only includes the main effects of the variables $(x_1, \ldots, x_k)$. It is often found, however, that both interaction between the variables and curvature of the response surface itself necessitates the development of the main effects model via a Taylor series expansion. This approach leads to the inclusion of higher order and interactive terms. Thus, a second-order model could be of the type

$$y = \beta_0 + \beta_1 x_1 + \beta_2 x_2 + \beta_{11} x_1^2 + \beta_{22} x_2^2 + \beta_{12} x_1 x_2 + \beta_{13} x_1 x_3 + \epsilon. \tag{5}$$

This particular model comprises three variables $x_1$, $x_2$, $x_3$, squared terms $x_1^2$, $x_3^2$ and interaction terms $(x_1x_2)$, $(x_1x_3)$. There are, therefore, a number of steps in the development of the RSM model, shown in generalized form in figure 1. The designed experiments to generate the data are described in the individual application sections. In both cases, the experimental procedure was followed to generate a training set to perform the model identification and fitting. The procedure was then repeated in each case to capture an unseen data set upon which to assess the accuracy of the model. Validation of the models was conducted upon this unseen data in all cases. Considering first the coefficient selection block, the appropriate model coefficients are selected by least-squares regression analysis. The algorithm may be extended to analyse any arbitrary order of the model, assuming sufficient computational resources are available for the processing of the data matrices.

For example, when considering a first-order model, the $\beta$ terms comprise the unknown parameter set which can be estimated by collecting experimental system data. These data can either be sourced from physical experiments or from previously designed dynamic computer models. The parameter set can be estimated by regression analysis based upon the experimental data. The method of least squares is typically used to estimate the regression coefficients. With $n > k$ on the response variable available, giving $y_1, y_2, \ldots, y_n$, each observed response will have an observation on each regressor variable, with $x_{ij}$ denoting the $i$th observation of variable $x_j$. Assuming that the error term $\epsilon$ has $E(\epsilon) = 0$ and

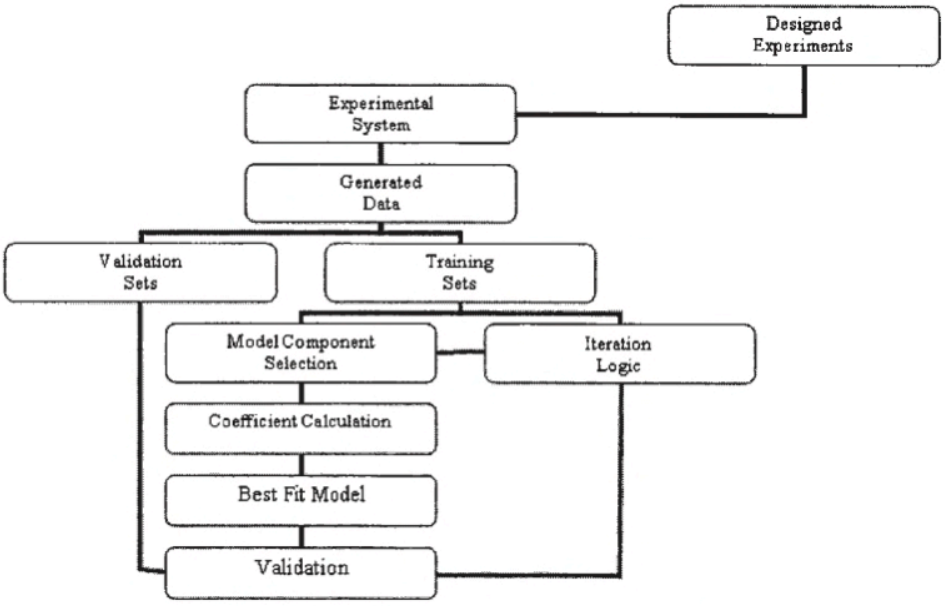


**Figure 1. Generalized flowchart for data-driven response surface modelling.**

$Var(\epsilon)=\sigma^2$ and the $(\epsilon_i)$ are uncorrelated random variables. The model can now be expressed in terms of the observations

$$\begin{aligned} y_i &= \beta_0 + \beta_1 x_{i1} + \beta_2 x_{i2} + \cdots + \beta_k x_{ik} + \epsilon_i \\ &= \beta_0 + \sum_{j=1}^{k} \beta_j x_{ij} + \epsilon_i, \\ i &= 1, 2, \ldots, n. \end{aligned} \tag{6}$$

The $\beta$ coefficients in equation (6) are chosen such that the sum of the squares of the errors $(\epsilon_i)$ are minimized via the least-squares function

$$\begin{aligned} L &= \sum_{i=1}^{n} \epsilon_i^2 \\ &= \sum_{i=1}^{n} \left( y_i - \beta_0 - \sum_{j=1}^{n} \beta_j x_{ij} \right)^2. \end{aligned} \tag{7}$$

The model can be more usefully expressed in matrix form as

$$\mathbf{y} = \mathbf{X}\beta + \epsilon, \tag{8}$$

where

$$\mathbf{y} = \begin{bmatrix} y_1 \\ y_2 \\ . \\ . \\ . \\ y_n \end{bmatrix}, \qquad \mathbf{X} = \begin{bmatrix} 1 & x_{11} & x_{12} & \ldots & x_{1k} \\ 1 & x_{21} & x_{22} & \ldots & x_{2k} \\ \vdots & \vdots & \vdots & \vdots & \vdots \\ 1 & x_{n1} & x_{n2} & \ldots & x_{nk} \end{bmatrix}$$

$$\beta = \begin{bmatrix} \beta_0 \\ \beta_1 \\ . \\ . \\ . \\ \beta_n \end{bmatrix}, \qquad \epsilon = \begin{bmatrix} \epsilon_1 \\ \epsilon_2 \\ . \\ . \\ . \\ \epsilon_n \end{bmatrix}. \tag{9}$$

It is now necessary to find a vector of least-squares estimators **b** which minimizes the expression

$$L = \sum_{i=1}^{n} \epsilon_i^2 = \epsilon'\epsilon = (\mathbf{y} - \mathbf{X}\beta)'(\mathbf{y} - \mathbf{X}\beta) \tag{10}$$

and yields the least-squares estimator of $\beta$ which is

$$\mathbf{b} = (\mathbf{X}'\mathbf{X})^{-1}\mathbf{X}'\mathbf{y} \tag{11}$$

and finally, the fitted regression model is

$$\hat{\mathbf{y}} = \mathbf{X}\mathbf{b}, \qquad \mathbf{e} = \mathbf{y} - \hat{\mathbf{y}}, \tag{12}$$

where **e** is the vector of residual errors of the model.

Model selection is performed by an iterative algorithm (figure 1) implemented as a Matlab script, which is initialized with the most basic model under consideration, a two input first order model:

$$\mu = \beta_0 + \beta_1 x_1 + \beta_2 x_2. \tag{13}$$

Least-squares fitting for the coefficients is performed, and the resulting model is run to predict the output of the validation data set. Confidence in the model is based upon the residuals vector. Supposing $n_i$ observations on the response of the $i$th level of the regressor $\mathbf{x}_i$, $i=1, 2, \ldots, m$, and $y_{i,j}$ represents the $j$th observation on the response at $\mathbf{x}_i$, $i=1, 2, \ldots, m$, and $j=1, 2, \ldots, n_i$. There are $n = \sum_{i=1}^{m} n_i$ total observations. The sum of squares ($SS_{lof}$) for lack of fit is

$$SS_{lof} = \sum_{i=1}^{m} n_i (y_i - \hat{y}_i)^2. \tag{14}$$

Interactive and higher-order components are successively added during each iteration until a predefined confidence level is reached according to the confidence metric $C$:

$$C = 100 - \left( \frac{SS_{lof}}{SS_y} \times 100 \right), \tag{15}$$

where $SS_y = \sum_{i=1}^{m} n_i (y_i)^2$, and $SS_{lof} < SS_y$. As an example of a higher order model which may be generated by the iterative process, a third-order candidate is considered.

$$\begin{aligned} \mu = {} & \beta_0 + \beta_1 x_1 + \beta_2 x_2 + \beta_{11} x_1^2 + \beta_{12} x_2^2 + \beta_{22} x_1 x_2 \\ & + \beta_{13} x_1 x_2^2 + \beta_{23} x_2 x_1^2 + \beta_{33} x_1^2 x_2^2 + \beta_{14} x_1^3 \\ & + \beta_{24} x_2^3 + \beta_{44} x_1^3 x_2^3. \end{aligned} \tag{16}$$

In this example, the basic linear model has been augmented during the iteration process by pure second- and third-order terms, as well as coupling terms. The model reflects the type of two input, single-output systems considered in this paper. However, systems exhibiting more degrees of freedom can be modelled using this technique.

## 3. Response surfaces and designed experiments for a computationally intensive distributed simulation

Complex systems such as aircraft can be represented by distributed simulations, requiring the development of administrative architectures necessary for the components to operate as a unified whole. Both common

object request broker architecture (CORBA), and the high level architecture (HLA) have been developed to provide a real-time simulation environment. Individual centres develop models that can subsequently join a distributed environment to construct a sophisticated representation with detail, accuracy and model flexibility at the component level. In particular, real-time flight simulators can be constructed with levels of detail focussing hierarchically down from the airframe flight characteristics, through aerothermal gas turbine engine models, to component models of fuel pumps, generators, etc. Distributed components of the system are on the whole modelled in high level environments such as Matlab/Simulink. Routines may also be coded in languages such as Fortran or C. The distributed simulation architecture registers the data types and protocols of these modelling environments, and provides channels for data streaming via a real-time kernel. The distributed architectures often rely on dedicated local (LAN) or wide (WAN) area networks to provide necessary physical levels of bandwidth for the data transfer. Finally, and most importantly, any individual component that runs slower than real-time will prevent the system from running in real-time if its operation is critical to the operation of the overall system. Many complex systems, particularly nonlinear multivariable ones, require in general intense computation in order to provide an accurate dynamic simulation. This problem is exacerbated by the use of high-level simulation packages to provide the model environment. Also, highly detailed techniques such as finite element analysis and computational fluid dynamics, by definition require large amounts of time to perform iterative solutions. Experimental data may be used to construct a model of the system, with the aim of constructing a representation accurate to known statistical bounds, with real-time capability and is developed here, as it has the advantages of a generic approach. Also, it lacks the disadvantages of increased hardware costs or increased system bandwidth requirement, while retaining the advantages of graphical development environments. The solution's effectiveness in application will be examined against both experimental and simulation data for a nonlinear permanent magnet AC (PMAC) motor drive (Stewart and Kadirkamanathan 1998, 1999). It is desired that the motor joins a distributed flight simulator as the actuator motive power for an electromechanical control surface actuator. In order to achieve the high velocities and torque required to achieve the operational bandwidth of the surface, a complex nonlinear model reference current controller is packaged in the simulation model (Stewart and Kadirkamanathan 2001) along with associated power electronics and feedback sensors (the simulation can be made more complex by the desired implementation of sensorless control). It is imperative that wherever possible, in order to maximize the useability and applicability of the flight simulator, that its response reflects, as closely as possible, the real-life dynamic response and interactions of the individual component parts. This allows the assessment and integration of new components and control systems in as 'real' an environment as possible. Thus, real-time integration and component level complexity are critical goals.

### 3.1. *Electrical drive system description*

A brief description will be presented to give an overview of the complexities of a PMAC motor and controller, and the level of computational overhead demanded by, for example, a Simulink model. The controller in question is a model reference type (Stewart and Kadirkamanathan 2001), which allows the torque speed envelope of the motor to be greatly increased. The general configuration of this class of motor is three phase AC, and a nonlinear transform (Park Transform) is usually applied to the phase currents and voltages to allow for easier analysis and control system design (Pillay and Krishnan 1989), to give the following description of the motor:

$$V_q = ri_q + \omega L i_d + \omega\lambda + L\left(\frac{\mathrm{d}i_q}{\mathrm{d}t}\right) \tag{17}$$

$$V_d = ri_d - \omega L i_q + L\left(\frac{\mathrm{d}i_d}{\mathrm{d}t}\right), \tag{18}$$

where $V_d$, $V_q$ are the $d$ and $q$ axis voltages, $i_d$, $i_q$ are the $d$ and $q$ axis currents, $r$ is the phase resistance, $\omega$ is the rotor velocity, $L$ the phase inductance and $\lambda$ the back EMF constant in the reference frame as volts/radian/second. The $q$-axis inductance is equivalent to the armature inductance, and the $d$-axis inductance is equivalent to the field inductance in a field wound DC machine. In the case of the surface mount PMAC motor considered here, these quantities are equal and are denoted by $L$. The $d$ and $q$ variables are obtained from the three phase quantities via the following definition of the Park transform

$$\begin{vmatrix} V_q \\ V_d \end{vmatrix} = \frac{2}{3}\begin{vmatrix} \cos(\theta) & \cos(\theta - 2\pi/3) & \cos(\theta + 2\pi/3) \\ \sin(\theta) & \sin(\theta - 2\pi/3) & \sin(\theta + 2\pi/3) \end{vmatrix} \begin{vmatrix} V_a \\ V_b \\ V_c \end{vmatrix}, \tag{19}$$

where $V_{a,b,c}$ are the three phase elements. This transformation also applies to current and flux linkage

quantities, and the three phase quantities may be obtained from the $d$ and $q$ axis variables by application of an inversion of the Park matrix in equation (19). High-performance phase current regulation is the key to high-performance motion control with the sinusoidal PMAC motor. Fast responding current regulation combined with self-synchronization via the built-in shaft position encoder make it possible to orientate the current phasor $I$ anywhere within the $d$–$q$ reference frame subject to supply current and voltage constraints:

$$V^2 \geq V_q^2 + V_d^2, \qquad I^2 \geq I_q^2 + I_d^2, \tag{20}$$

where $V$ is the available DC voltage magnitude and $I$ the absolute maximum current limit magnitude for dynamic operation. The speed of the torque response is limited only by the source voltage and stator inductance values. Torque production is a linearly related to $q$ axis current by the torque constant, thus:

$$T_e = k_t i_q. \tag{21}$$

*3.1.1. Model reference controller*. The baseline approach to torque control is to map the torque command $T_e^*$ into demands for the $d$ and $q$ axis currents. These current commands are then transformed into instantaneous sinusoidal currents for the individual stator phases, using the rotor angle feedback and the basic inverse vector rotation equations. PI current regulators for each of the three phases then excite the phase windings resulting in desired current amplitudes. Examination of the motor equations (17) and (18) reveals cross-coupling between the equations, which requires correction by a feedback linearizing controller to allow accurate control of the current and voltage vectors (Stewart and Kadirkamanathan 2000). The flux weakening controller supplies current commands based upon rotor velocity and torque demand, and is based upon the standard circle diagram representation (Jahns 1987, Miller 1993). As speed and frequency increase, the current limit locus remains fixed. However, the radius of the voltage limit locus decreases. The PWM control saturates when its duty cycle reaches maximum, and the available sinewave voltage from the inverter equals the phase voltage. This operating point is known as 'base speed' and occurs on the circle diagram at the intersection of the $q$ axis, current limit circle and voltage limit circle, If the rotor velocity increases further, the radius of the voltage-limit circle decreases further, and maximum current is defined by a current vector terminating in the intersection of the two circles. As rotor velocity increases, the voltage-limit circle drags the current phasor further and further ahead of the $q$ axis, decreasing the torque producing current, and increasing the demagnetizing negative $d$ axis current. This acceleration can increase until the point where the current vector lies entirely in the demagnetizing direction, and no further torque production is possible. The motor and controller models are coded into Simulink models, together with function blocks to describe real system objects such as the three-phase PWM inverter, feedback linearizing controller, rotor position encoder, Park transform blocks and blocks to describe the voltage drop due to the current dynamics (Stewart and Kadirkamanathan 1998). An external PID actuator position control loop supplies torque demand signals to the PMAC motor and controller simulation. However, when the Simulink model of the model reference control system was run on a Pentium III 800 MHz computer with 512 Mb system memory, it was found not to be capable of real-time operation, running outside wall clock time by a factor of five at the required sampling rate of 1 kHz. It was thus decided to implement a model of the controller by RSM in order to achieve real-time status for the motor/controller simulation.

### 3.2. *RSM modelling of the model reference controller*

The model reference controller can be converted into a response surface by viewing it as an input–output model. In this respect, the input variables are rotor velocity and torque demand, while the output variable is the angle of current vector advance. The nature of this approximation is to a large extent steady state, although its effect when implemented is dynamic. The designed experiment collects data from the dynamometer when all transients have decayed to zero in order to find the highest torque available at the operating point under consideration. Hence, in this case, the model represents a map of steady-state operating points. When the approximation is applied as a controller. However, the identified polynomial acts as a model reference to a system which is operating both dynamically and in steady state. This is possible, since in a modern well-designed PMAC motor, the phase inductance $L$ (equations (17) and (18)) is small, and also in fact, the rate of advance with respect to time of the current vector in the flux weakening region is restricted when driving realistic load torques. Hence, the unmodelled voltage drop due to the current dynamics can be assumed to be zero, particularly in this case where the motor is driving a large inertial load. A factorial approach to experimental analysis on a four quadrant dynamometer was adopted (Hicks and Turner 1999) to populate the three-dimensional response space. An initial approach to deriving this population would be to combine each increment of PWM modulation depth with each increment of velocity

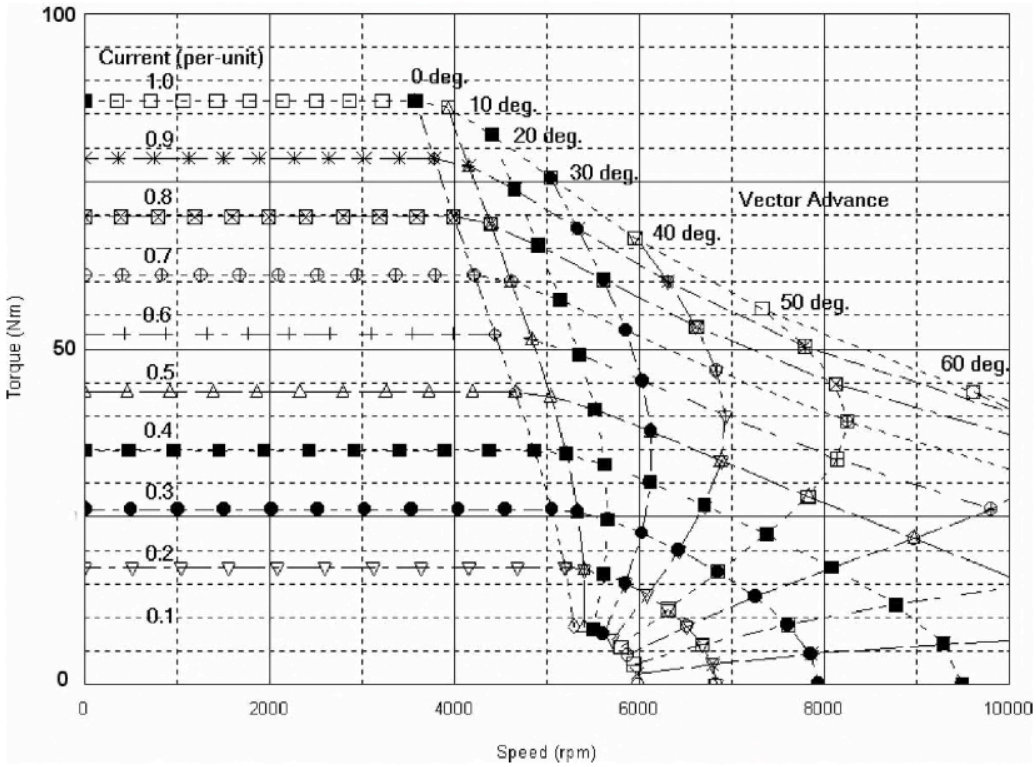


**Figure 2. Torque speed–current vector advance experimental data.**

to give the output torque surface. This would result in an output space (figure 2) with 180 experimental data points (all the points present in figure 2). The operational space of the motor can however, be divided into linear and nonlinear regions, by populating the map in terms of modulation depth and angle of current vector advance. This results in the linear region being defined by data points at the start and finish of the linear region for each modulation depth. The nonlinear region is defined by data points at 10° increments for current vector advance at each level of modulation depth. This factorial approach reduces the number of experimental data points to be collected to 90, an advantage of 50%. Modulation depths 0.3 and 0.4 have black squares across the linear region to indicate the range of experiments which have been eliminated. Before the experimental procedure was carried out, each datum point was assigned a series number between 0 and 90. The order of experimentation was decided via a random number generator in Matlab, according to experimental design procedures (Hicks and Turner 1999). The characterization study was conducted on a dynamometer rig. The method is to map the surface that describes the surface connecting torque, rotor velocity and current vector advance. The mapping is conducted for a quantization of 10° current vector advance, and PWM modulation depth from 0 to 100% in increments of 10%. The PWM modulation depth is given as per unit current on the left hand side of figure 2. The RSM is utilized to construct a response surface that reflects the current advance profile in the flux-weakening region of the motor. The natural units $\xi_1$ (instantaneous torque in Nm) and $\xi_2$ (rotor velocity in rads/s) of the experimental dynamometer data is first transformed into the corresponding coded variables $x_1$ and $x_2$, such that

$$x_{i1} = \frac{\xi_{i1} - [\max(\xi_{i1}) + \min(\xi_{i1})]/2}{[\max(\xi_{i1}) - \min(\xi_{i1})]/2} \tag{22}$$

and

$$x_{i2} = \frac{\xi_{i2} - [\max(\xi_{i2}) + \min(\xi_{i2})]/2}{[\max(\xi_{i2}) - \min(\xi_{i2})]/2}. \tag{23}$$

The second-order model (order and structure ascertained by the iterative procedure described in Section 1) to be fitted to the data was:

$$\begin{aligned} y = {} & \beta_0 + \beta_1 x_2 + \beta_2 x_2 + \beta_{11} x_1^2 \\ & + \beta_{22} x_2^2 + \beta_{12} x_1 x_2 + \epsilon. \end{aligned} \tag{24}$$

Using equations (10)–(13), we obtain the coefficient matrix:

$$b = \begin{bmatrix} 38.19 \\ 25.46 \\ -7.28 \\ -11.04 \\ 6.23 \\ -5.84 \end{bmatrix}. \tag{25}$$

Therefore, the model of the flux weakening surface is

$$\begin{aligned} \hat{y} = {} & 38.19 + 25.46x_1 - 7.28x_2 - 11.04x_1^2 \\ & + 6.23x_2^2 - 5.85x_1x_2, \end{aligned} \tag{26}$$

which may be slightly biased if the noise is coloured. The expression for the response surface model can now be implemented as a controller in Simulink and the performance compared with the original Simulink model.

## 4. Response surfaces for rapid prototyping of an automotive control system

We will now consider the development of a low-cost electronic throttle actuator, and microcontroller development to control vehicle oscillation. 'Drive-by-wire' applications for the replacement of the conventional cable link between the throttle pedal and the throttle body are the focus of development by many major automotive manufacturers. By fitting a stepper or permanent magnet servo motor (Stewart and Kadirkamanathan 1998) to the throttle body, and an electronic throttle pedal with potentiometer, a drive-by-wire system can be implemented. Control systems have been designed (Rossi *et al.* 2000), which allow fast and accurate response to changes in pedal demand, and have been shown to possess robust operating characteristics. The initial requirement is to damp the acceleration oscillations generated by throttle step changes. This mapping is constrained by the requirement to maximize the vehicle acceleration response available to the throttle. Control analysis and design for this automotive system is complicated by a number of factors. There are a number of nonlinearities present such as backlash in the gearbox, a tyre model which varies nonlinearly which load, and nonlinear clutch response. Also there exists a process lag between throttle actuation and torque production and nonlinear engine torque-speed mapping.

### 4.1. *Data acquisition and system description*

Experimental data were available from a test car which was fitted with a data acquisition system including three axis accelerometers, and had been loaned for the purpose of analysis, design and testing. The feasibility of the proposed designed experiment was initially performed in simulation (figure 3), and subsequently a systematic excitation of the driveline was made experimentally on the vehicle by performing step demands in all gears at discrete points throughout the effective engine speed range of the vehicle. The generated experimental data (road speed, acceleration, engine speed, etc.) were analysed using the RSM. In the development of a model and control system constrained by computational considerations, and the requirement of rapid prototyping, the RSM allows a low-order approximation to be derived from the available empirical data (Stewart and Fleming 2001). A reduced-order representation can then be employed in the controller. Application of the RSM analysis to the vehicle response data allows a system model to be developed that lends itself to the design of a scheduled controller structure which is shown to control the first torsional mode of the driveline. Dynamic models of the driveline and engine are widely available, ranging from simple linear models to highly complex nonlinear models. To illustrate the complexity of the control problem, a nonlinear model is presented here that addresses the driveshaft flexibility and adds certain nonlinear elements. A high-order nonlinear model is obtained which in tandem which other factors such as engine lag and unidirectional torque production, shows the difficulties of designing a controller for this system. The driveline can be modelled (Kienke and Nielsen 2000) as a system comprising engine (flywheel), clutch, transmission, propshaft (in the case of rear wheel drive vehicles), final drive, driveshafts, wheels and tyres, and vehicle mass, giving (for the nomenclature, see the appendix):

$$J_e\ddot{\theta}_c = T_e - T_{fe} - M_{kc}(\theta_c - \theta_t i_t) - d_c(\dot{\theta}_c - \dot{\theta}_t i_t) \tag{27}$$

$$\begin{aligned} & \left(J_t + \frac{J_f}{i_f^2}\right)\ddot{\theta}_t \\ & = i_t\left(M_{kc}(\theta_c - \theta_t i_t) + d_c(\dot{\theta}_c - \dot{\theta}_t i_t)\right) \\ & \quad - \left(d_t + \frac{d_f}{i_f^2}\right)\dot{\theta}_t - \frac{1}{i_f}\left(k_d\left(\frac{\theta_t}{i_f} - \theta_w\right) + d_d\left(\frac{\dot{\theta}_t}{i_f} - \dot{\theta}_w\right)\right) \\ & (J_w + mr_e^2)\ddot{\theta}_w = k_d\left(\frac{\theta_t}{i_f} - \theta_w\right) + d_d\left(\frac{\dot{\theta}_t}{i_f} - \dot{\theta}_w\right) \\ & \quad - (d_w + mc_{r2}r_e)\dot{\theta}_w - \frac{1}{2}c_a A_v \rho_a r_e^3 \dot{\theta}_w^2 - r_e m(c_{r1} + G\sin(\tau_r)). \end{aligned} \tag{28}$$

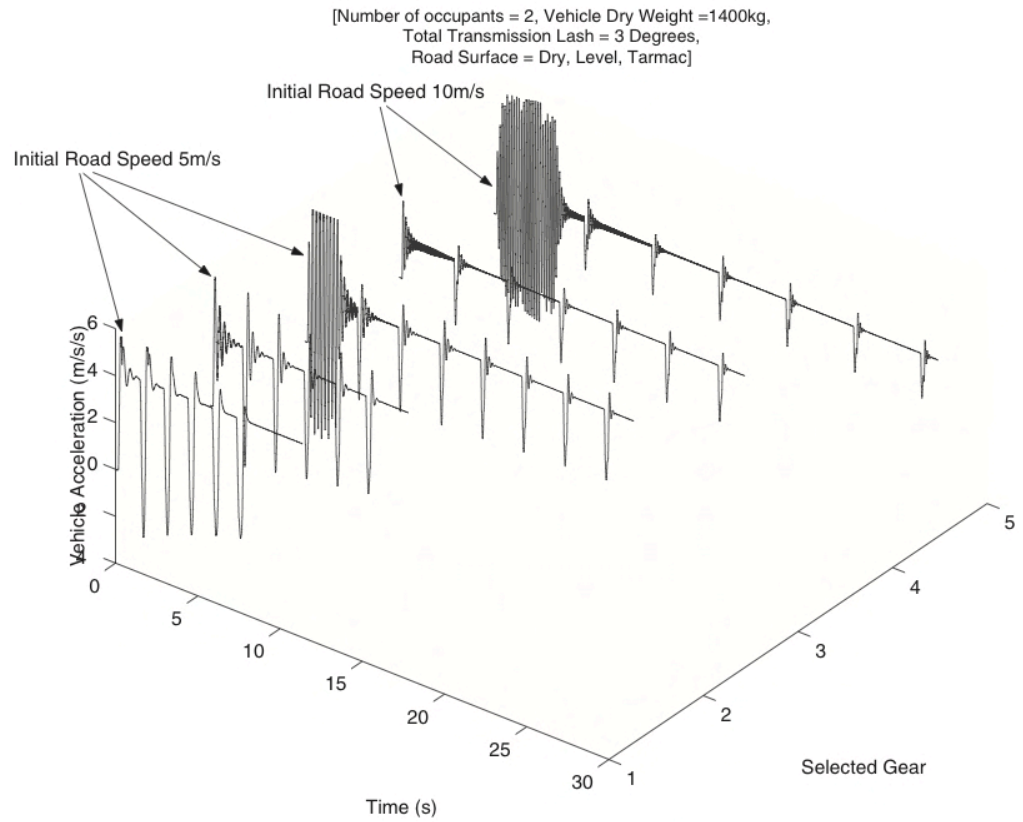


**Figure 3. Simulation of the designed step response experiment before road-tests.**

This high-order representation of the system gives a reasonable response when implemented as a simulation and compared with experimental responses. It does differ from the real system in significant respects, however. The first difference is the presence of backlash in the geared elements such as the gearbox and differential. This effect is manifest as a deadzone at tip-in while the transmission angular slack is taken up during the application of engine torque. This will also contribute nonlinear effects during transmission oscillations after the initial tip-in torque transient. Second, the tyre model (Burkhardt 1993) in reality is far more complex than the description in the given model in terms of wheel slip and friction coefficient.

### 4.2. *Designed experiments and RSM modelling*

In contrast to the aerospace application described previously, the approximation derived here encompasses both steady-state and dynamic responses. The polynomial approximates the system as characterized by its damping ratio. In this way, the behaviour of the vehicle is mapped according to its response to a step throttle input in terms of rise time, settling time and overshoot. In the analysis of the acceleration response of the vehicle, there are three variables of interest, namely vehicle loading, road speed and selected gear ratio. For the purpose of clarity in the description, vehicle loading will be assumed to be a fixed standard two person loading of 160 kg. In order to reduce the overall number of data sets required to construct the response surface of the system, a factorial approach (Hicks and Turner 1999) is adopted. The combinations of factorial experiments at $5\,\mathrm{ms}^{-1}$ in each gear requires 25 experiments to be performed. Each proposed factorial combination was assigned a serial number and performed in random order via output from a random number generator. Each experiment consists of coasting the vehicle in the appropriate gear at the appropriate roadspeed, and performing a 100% tip-in with the accelerator pedal. This corresponds to exciting the open loop system with a unit step torque input. On the day of testing, the 1 mile asphalt test road was dry, with overcast sky and ambient temperature of 60 °F. The effect of the energy storage components in the driveline can be clearly seen in an examination of the vehicle at $10\,\mathrm{ms}^{-1}$ in second gear in figure 4. Examination of the vehicle response to tip-in reveals a system that can be approximated as a delay and second-order dynamic response with an overshoot and

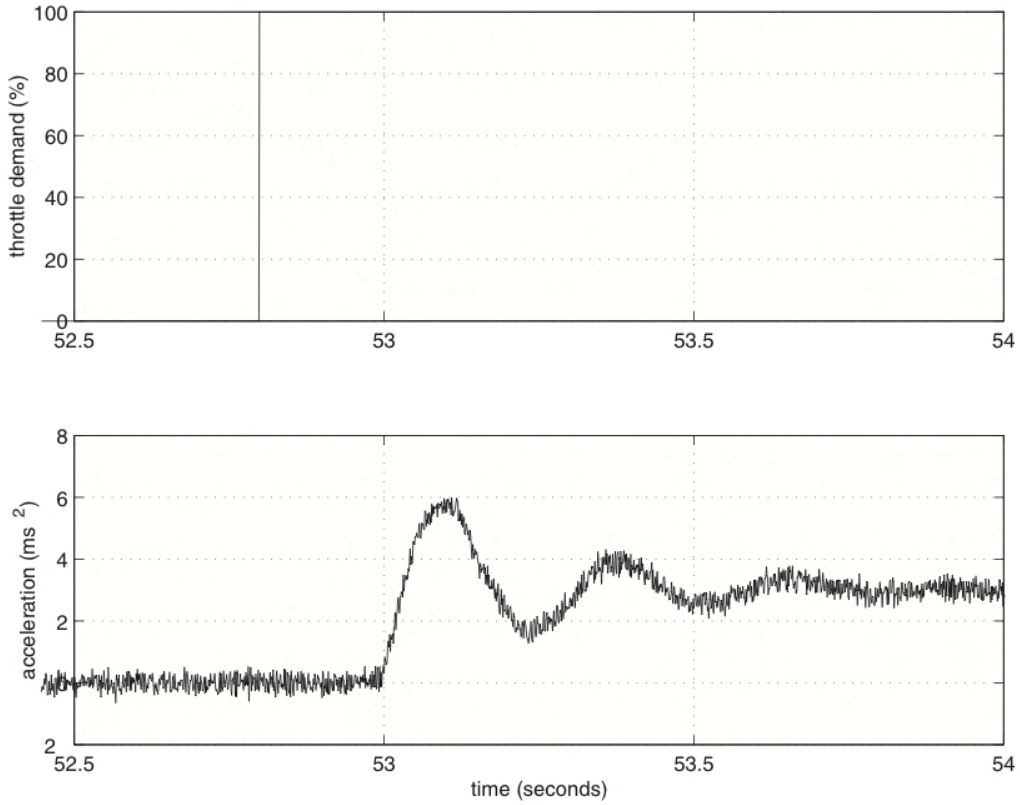


**Figure 4. Vehicle acceleration response (b) in second gear at 10 ms$^{-1}$ to throttle step demand (a).**

settling time which varies with road speed and selected gear. This approximation to describe the entire vehicle response can be formulated by application of RSM to the experimental data. Of note is also the lag between actuation and response. The torque lag is combined with a high level of lash for this high mileage vehicle. The experimental data that has been gathered can be synthesized into a response map for the vehicle in order to design an oscillation control system. For the definition of driveability under consideration here, the vehicle response can be characterized as the damping ratio of the second-order approximation map with variables road speed and selected gear. The individual experimental responses may be expressed in terms of overshoot and settling time. The transfer function describing the open loop system may be described as:

$$\frac{C(s)}{R(s)} = k\frac{1}{as^2 + bs + c}, \tag{29}$$

from which the damping ratio of the system can be calculated as the ratio of the actual damping $b$ to the critical damping $b_c = 2\sqrt{ac}$ (Ogata 1990). Thus, the damping ratio $\zeta$ can be calculated from $\zeta = b/b_c$. The roots of the characteristic equation (29) are $s_1, s_2 = -b_c \pm jc\sqrt{1 - b_c^2}$. This forms a complex conjugate pair from which the damping ratio and natural frequency can be computed. The natural units $\xi_1$ (road speed in miles per hour) and $\xi_2$ (selected gear) of the experimental data are first transformed into the corresponding coded variables $x_1$ and $x_2$, such that

$$x_{i1} = \frac{\xi_{i1} - [\max(\xi_{i1}) + \min(\xi_{i1})]/2}{[\max(\xi_{i1}) - \min(\xi_{i1})]/2} \tag{30}$$

and

$$x_{i2} = \frac{\xi_{i2} - [\max(\xi_{i2}) + \min(\xi_{i2})]/2}{[\max(\xi_{i2}) - \min(\xi_{i2})]/2}. \tag{31}$$

This is a coding scheme widely used in fitting linear regression models, resulting in the values of $x_1$ and $x_2$ falling between $-1$ and $+1$. Thus, the response surface in terms of the coded variables is obtained via a model which had been identified by the iterative procedure described in Section 1. The best fit model was found to have an identical second-order structure to that identified for the aerospace application (equation 24).

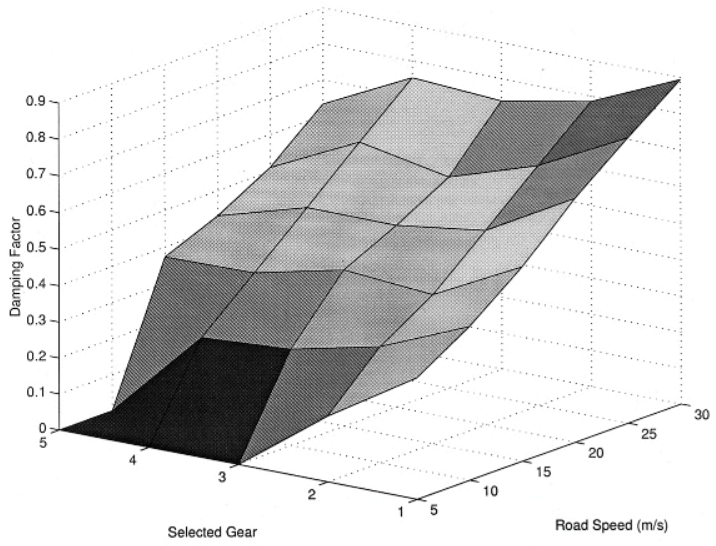


**Figure 5. Vehicle damping ratio response surface.**

The equation describing the response surface in this case was found to be

$$\hat{y} = 0.4079 - 0.804x_1 + 0.3809x_2 + 0.0519x_1^2 - 0.0429x_2^2 - 0.0121x_1x_2. \quad (32)$$

This can be converted back into an equation using the natural variables by reversing the conversion process in equations (31) and (32). Comparing the computed response surface against a second experimental data set gave an average residual error of 1.65%. The surface as fitted in terms of damping ratio, selected gear and road speed is shown in figure 5. The gear numbers in figure 5 correspond to a standard 2.5-litre V6 Ford Mondeo gearbox. Interpolation between the gears allows an approximation to be made which predicts the response of gearboxes with alternative individual ratios, should the controller be applied to a non-standard vehicle.

The control of driveline shuffle has been the subject of controller design, including LQR and generalized optimal control (Best 1998) noting that the technique is 'unlikely to prove beneficial in any practical implementation of driveline control', and pole placement (Richard *et al.* 1999a), which utilizes a ninth-order controller which although damping the decay oscillations, adds an undesirable initial acceleration transient. As noted, it is required to assess the usefulness of RSM for rapid prototyping and also to provide an initial simple useable controller to identify the potential of the electronically operated throttle body for controlling the driveline. The simple feedforward controller is designed as follows. A response surface has been obtained (figure 5) which describes accurately the vehicle's damping ratio map. As an initial design target, a damping ratio of 0.7 across the entire operating map would be a desirable response. The problem as presented to the control designer is nonlinear and time variant (varying with selected gear and roadspeed), a transport delay exists in terms of engine torque production, and the engine torque output varies nonlinearly in terms of engine speed, engine temperature and other factors. The RSM analysis, however, allows a simple open loop feedforward controller to be immediately designed and implemented to allow a fast appraisal of the actuator potential. The system response surface extracted from the experimental data is a representation of the complex conjugate pole pairs of the approximation in terms of the system's varying damping ratio. The initial approach will be to effect a pole-zero cancellation of these complex conjugate poles by utilizing the damping ratio response map, and pole placement to give a satisfactory response, by utilizing the damping ratio error response map. This method does rely on accurate knowledge of the position of the uncompensated poles which has been ascertained experimentally for the purpose of this development. The parameters of the feedforward controller are derived in real-time from the response surface and are a function of selected gear and roadspeed. The feedforward compensator takes the form $as^2 + bs + c/as^2 + ds + c$, where the coefficient $b$ is calculated from the damping ratio response surface, and performs pole-zero cancellation. Coefficient $d$ produces the desired pole placement and forms the requires damping ratio, and is calculated from the sum of the damping ratio response surface, and the damping ratio response error surface. The demand from the throttle pedal, throttle position and roadspeed were read in via A/D ports, and the selected

gear read in via the digital I/O. Output from the controller was sent to a power amplifier via the PWM port. With the controller in place, the experimental set was repeated to assess the potential of the electronic throttle control.

## 5. Results

It is now possible to assess the performance of the data-driven modelling procedure.

### 5.1. *Distributed aerospace simulation*

In the case of the distributed simulation, by connecting the model reference controller and second-order response surface model in turn to the existing PMAC motor and actuator driven model, the output can be compared with existing experimental data sets. In this experiment (figure 6), the motor is accelerating from rest and run up to a rotor velocity of approximately 7500 rpm. This is a particularly arduous operating envelope, as the motor is being simulated with a coarse position feedback encoder rather than the more usual high-resolution encoder. This is responsible for the high level of ripple in the torque envelope. A visual inspection of the torque profiles produced by the two controllers reveals little or no difference in performance of the accelerating motor. The controller command outputs were found to have a mean difference of less than 1°, which reflects the mean error in the initial controller design from experimental data, where the mean error of the second order fit was also $< 1°$. The simulations were repeated for verification over a number of randomly chosen profiles over the entire torque/speed range. The error bounds were found to be $< 1°$ in all simulations. The second-order controller obtained through the RSM was found to operate at more than 10 times wall-clock time compared with the original Simulink controller which could not attain real-time operation. The increase in performance ($> 50$ times) was such that it was possible to run the rudder motor and controller on the same machine in real-time without any modifications to the motor-drive simulation, which is in itself a valuable improvement. The final implementation was to run the RSM designed controller on a separate machine from the motor and drive to confirm its benefits for distributed simulations. The simulation ran via a 100 Mb/s LAN via standard network interface cards, and bespoke data buffers

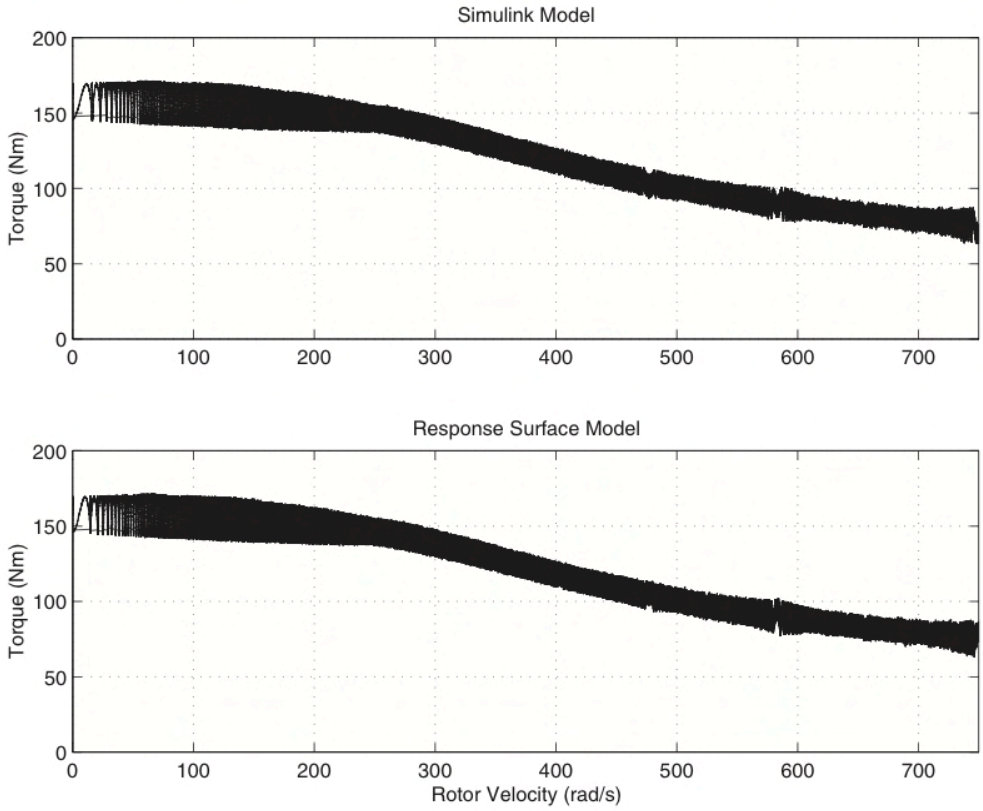


**Figure 6. Comparison of Simulink and RSM controllers in motor acceleration simulation.**

and sockets programmed in both C++ and Visual Basic. No buffer under-runs were experienced, and the controller was found to stream data successfully in real-time, operating at 1 kHz under the HLA.

### 5.2. *Automotive rapid prototyping application*

In the other example, the goal of rapid prototyping was achieved in a matter of days between initial experimental testing and final implementation testing. The original set of experiments were repeated with the electronic throttle both compensated and uncompensated. A comparison at the $10\,\mathrm{ms}^{-1}$ in second gear step response is shown in figure 7. The time axis in both traces was zeroed at the initiation of the step demand for the purpose of clarity. The marked improvement in vehicle oscillation obvious in figure 7 was repeated throughout the operating map of the vehicle. The compensated vehicle responses over the operating region of the vehicle were found to have a mean damping ratio of 0.68, with a maximum residual of 0.07. The tip-in driveability of the vehicle was found to be subjectively improved, in addition to the experimental evidence of the vehicle damping ratio map. Although a small amount of acceleration rate is sacrificed to achieve the suppression of oscillations, subjectively the vehicle's performance was not felt to be affected during appraisal by a group of four drivers, an appraisal carried out on a standard closed road route with the controller alternatively switched in and out.

## 6. Conclusions

A method has been presented that has been adapted from process control and optimization methodologies. For real-time distributed simulation environments, the approach allows the adaptation of complex aerospace controllers and systems which are too slow to join real-time simulations to be approximated in a way such that real-time simulation becomes possible. The method has been demonstrated on a PMAC flux weakening controller for a rudder actuator and found to provide not only the performance boost in terms of run-time, but also the accuracy required by the simulation environment. The method is shown to be a useful tool in the development of complex real-time systems.

The method is capable of finding polynomials of higher order than 1 or 2 if necessary. However, it

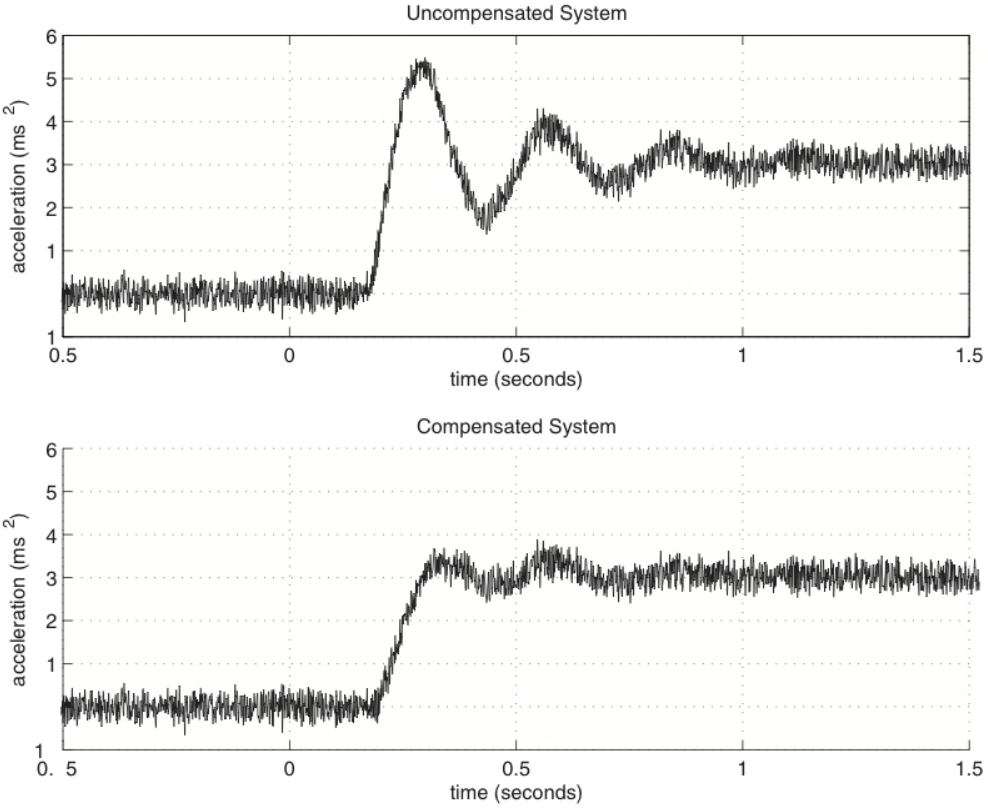


**Figure 7. Vehicle compensated and uncompensated step response.**

was found in the two diverse, demanding applications presented here (and other engineering applications not described due to lack of space) that in fact order 2 was sufficient. The iterative search engine attempts to find a good fit with the minimum number of regressors. The technique that has its roots in process control was found to be successful where other techniques such as LQR, etc. were found to be unsuccessful.

The experiments to generate the data were designed to produce well behaved (not too much, not sparse, not localized) data sets. It was not obvious in either case that the solutions would be of low dimension in terms of model order, it was co-incidental that both were capable of modelling as second-order polynomials. It is necessary to identify the dominant inputs to the system. In the automotive case, the inputs could be extended to include wind speed, wind direction, tyre pressures, engine temperature, etc. However, the fundamental system is a two-input single-output system. By coincidence the aerospace application was also identified fundamentally as a two-input single-output system. The technique can cope with higher orders of inputs.

The experimental datasets generated for the applications were inherently extremely noisy due to the use of high-frequency switching power electronic drives, etc. The use of recursive least squares to identify the model parameters, and careful use of analogue and digital filters on the data acquisition system to a greater extent circumvent the problems associated with noise. Designed experiments have been implemented in this paper to populate regularly the entire operational envelopes of the systems under consideration, so again the problems associated with sparse data are circumvented.

In the real-time automotive application, two hierarchically related objectives, first, to examine the application of the RSM to rapid control design prototyping, and having successfully achieved this goal, the second objective was to use the RSM to examine the potential of electronic throttle control to shape the acceleration response of an experimental vehicle. A controller based on nonlinear techniques and certain aspects of pole placement was eventually developed, but the timescale for analysis and design available for this project being particularly stringent, proved the usefulness of the RSM technique. The benefits of its addition to the controller designer's toolbox become immediately apparent when we consider the design process presented here. The timescale from experimental data captured through RSM analysis to experimental verification and assessment of the electronic throttle's potential for vehicle acceleration shaping was under 4 days. At this point, a judgement upon the viability and potential of the project could easily be made with confidence. In parallel with the RSM analysis, standard controller designs were being implemented and assessed. However, these designs are still in the development stage after many months. In conjunction with the existing mathematical models of the vehicle driveline presented in Section 5, it is necessary to develop a fully dynamic model in a software simulation package such as Simulink. The development of the mathematical models in conjunction with a simulation and also highly complex nonlinear controller design is by its nature an extremely time consuming task. In this context, the use of the RSM becomes extremely attractive. The technique has allowed an examination of the system control potential to be made at the start of the project, benefiting both the confidence of the industrial partners, and giving a realistic benchmark of potential performance. The controller derived by the RSM is immediately useable on the experimental vehicle, providing a demonstration facility at project inception. Some other benefits of this development tool are also significant. A controller is quickly available for verifying the computational, mechanical and electrical components of the control system, giving a stable platform for subsequent controllers as and when they become available. The controller as designed via the RSM is simple and low order by nature, and thus can be installed on a very simple microcontroller. Finally, a quick and cheap assessment of a system's potential can be rapidly made in order to support project development proposals. A controller has been developed to examine the potential of electronic throttle control. The stated requirements were rapid prototyping algorithm simplicity in both design and implementation, oscillation control, and the ability to work effectively across the entire operating region of the vehicle. All these requirements have been fulfilled, with the conclusion that electronic throttle control is a capable tool in a suite of applications to control the various aspects of 'driveability'. A secondary achievement has been to implement the control system on extremely cheap widely available components, further adding to its attractiveness to the automotive industry. A design method has been followed, centered around the RSM which has enabled the rapid prototyping process from empirical data. The design of a useable implementation has been achieved on a time varying process with significant time delays and nonlinearities.

The advantages to be gained by the application of data driven modelling has been shown in two disparate applications. For the real time distributed simulation case, it has been made possible for the representation derived from a computationally intensive simulation to attain real-time performance. For the automotive control case, the multiple goals of rapid prototyping, and hardware verification are achieved alongside the design of a computationally extremely efficient acceleration oscillation controller.

## Acknowledgements

The authors acknowledge the Department of Trade and Industry (DTI) CARAD programme, and the Ministry of Defence's (MOD) Corporate Research Programme for funding.

## Appendix

*Physical variables*

- $J$ moment of inertia,
- $\theta$ angular position,
- $T$ torque,
- $M$ mass,
- $d$ damping coefficient,
- $i$ gearing ratio,
- $k$ spring stiffness,
- $m$ mass,
- $r$ effective rolling radius,
- $G$ acceleration due to gravity.

*Subscripts*

- $e$ engine,
- $c$ clutch,
- $fe$ engine friction,
- $t$ transmission,
- $f$ friction torque,
- $d$ differential,
- $w$ wheel,
- $a$ aerodynamic drag,
- $\rho$ air density.

## References

BEST, M. C., 1998, Nonlinear optimal control of vehicle driveline vibrations. *UKACC International Conference on Control'98*, Swansea, 1–4 September 1998, pp. 658–663.

BURKHARDT, M., 1993, *Fahrwerktechnik: Radschlupf — Regelsysteme* (Wurtzburg: Vogel Fachbuch).

HICKS, C. R., and TURNER, K. V., 1999, *Fundamental Concepts in the Design of Experiments* (Oxford University Press: New York).

JAHNS, T. M., 1987, Flux weakening regime operation of an interior permanent magnet synchronous motor drive. *IEEE Transactions on Industrial Applications*, **1A–23**.

KIENCKE, U., and NIELSEN, L., 2000, *Automotive Control Systems* (Berlin: Springer).

MILLER, T. J. E., 1993, *Brushless Permanent Magnet and Reluctance Motor Drives* (EUCA, Grenoble: University Press).

MYERS, R. H., and MONTGOMERY, D. C., 1995, *Response Surface Methodology: Process and Product Optimization Using Designed Experiments* (New York: Wiley).

OGATA, K., 1990, *Modern Control Engineering* (New York: Prentice-Hall).

PILLAY, P., and KRISHNAN, R., 1989, Modelling, simulation and analysis of permanent magnet motor drives, Part 1: The permanent magnet synchronous motor drive. *IEEE Transactions on Industrial Applications*, **25,** 265–273.

RICHARD, S., CHEVREL, P., and MAILLARD, B., 1999a, Active control of future vehicles drivelines. *38th IEEE Conference on Decision and Control* (Piscataway: IEEE), Vol. 4, pp. 3752–3757.

RICHARD, S., CHEVREL, P., DE LARMINAT, P., and MARGUERIE, B., 1999b, Polynomial pole placement revisited: application to active control of car longitudinal oscillations. *1999 European Control Conference*, Karlsruhe, Germany.

ROSSI, C., TILLI, A., and TONIELLI, A., 2000, Robust control of a throttle body for drive by wire operation of automotive engines. *IEEE Transactions on Control Systems Technology*, **8**.

STEWART, P., and FLEMING, P., 2001, The Response Surface Methodology for real-time distributed simulation. In *IFAC Conference on New Technologies for Computer Control*, Hong Kong, China, 19–22 November 2001.

STEWART, P., and KADIRKAMANATHAN, V., 2001, Dynamic model reference PI control of flux weakened permanent magnet AC motor drives. *IFAC Journal of Control Engineering Practice*, **9,** 1255–1263.

STEWART, P., and KADIRKAMANATHAN, V., 1998, On steady state and dynamic performance of model reference control for a permanent magnet synchronous motor. *UKACC International Conference on Control 98*, 1–4 September, 1998. University of Wales, Swansea, pp. 664–669.

STEWART, P., and KADIRKAMANATHAN, V. 1999, Dynamic control of permanent magnet synchronous motors in automotive drive applications. *1999 American Control Conference*, San Diego, 2–4 June 2000, pp 1677–1681.

STEWART, P., and KADIRKAMANATHAN, V. 2000, Dynamic model reference control of a PMAC motor for automotive traction drives. *UKACC International Conference on Control 2000*, Cambridge, UK, 4–7, September 2000.